

# From Statistical Mechanical Models to Tensor Network Decoding

Christopher Chubb

Université de Sherbrooke

Stat Mech Mapping: arXiv:1809.10704, to appear in AIHPD  
with Steve Flammia

Tensor Network decoding: To appear arXiv:2009:?????

Passive error correction: physics alone suppress errors

Active error correction: decoder needed to remove error

Two classes of decoder:

- Practical decoders: Speed over accuracy
- Analytic decoders: Accuracy over speed

Passive error correction: physics alone suppress errors

Active error correction: decoder needed to remove error

Two classes of decoder:

- Practical decoders: Speed over accuracy
- Analytic decoders: Accuracy over speed

Passive error correction: physics alone suppress errors

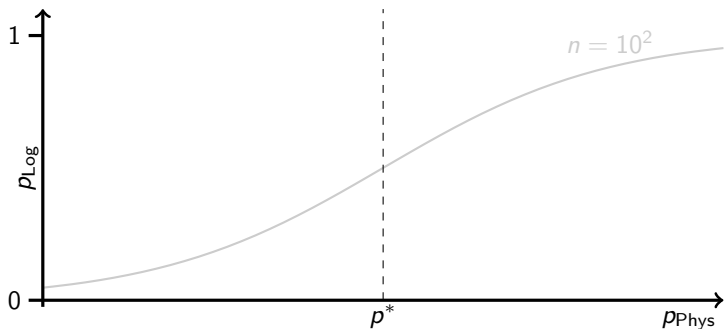
Active error correction: decoder needed to remove error

Two classes of decoder:

- Practical decoders: Speed over accuracy
- **Analytic decoders: Accuracy over speed**

# Threshold

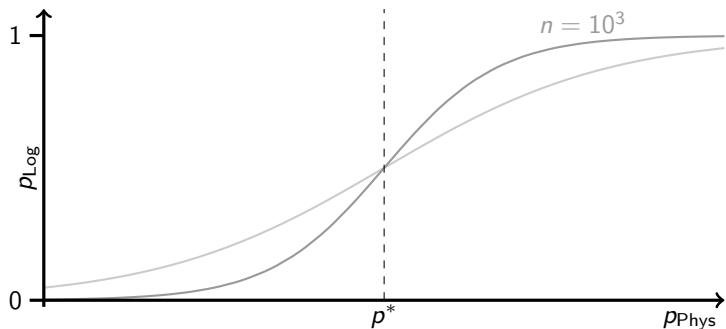
For large system sizes, performance is largely described by the threshold.



The inherent performance of the code can be studied by considering the optimal decoder.

# Threshold

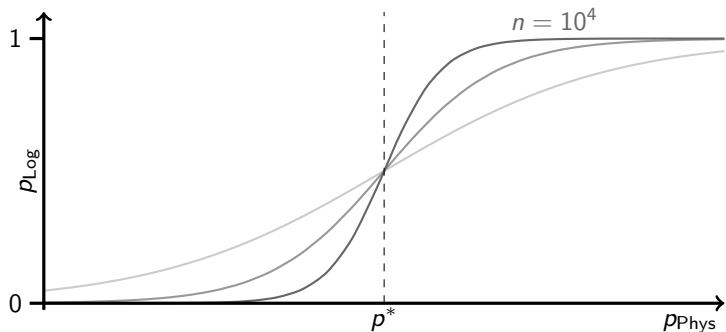
For large system sizes, performance is largely described by the threshold.



The inherent performance of the code can be studied by considering the optimal decoder.

# Threshold

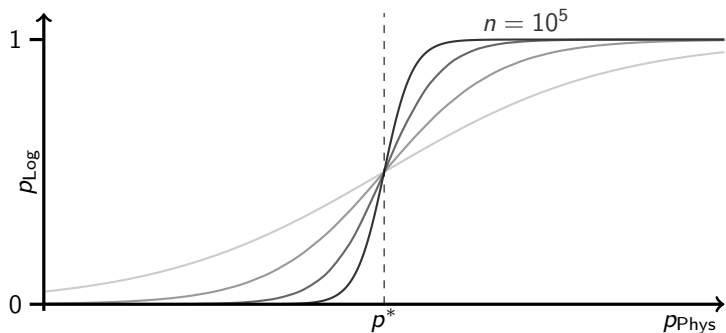
For large system sizes, performance is largely described by the threshold.



The inherent performance of the code can be studied by considering the optimal decoder.

# Threshold

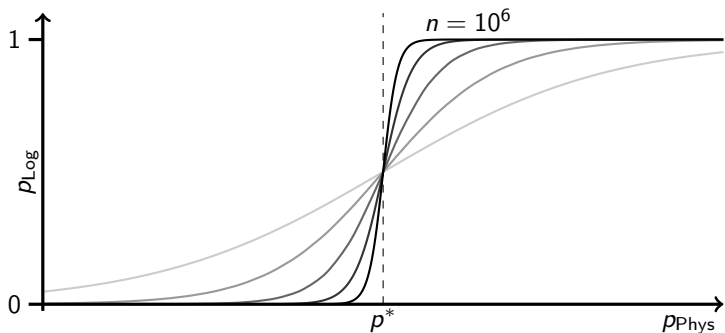
For large system sizes, performance is largely described by the threshold.



The inherent performance of the code can be studied by considering the optimal decoder.

# Threshold

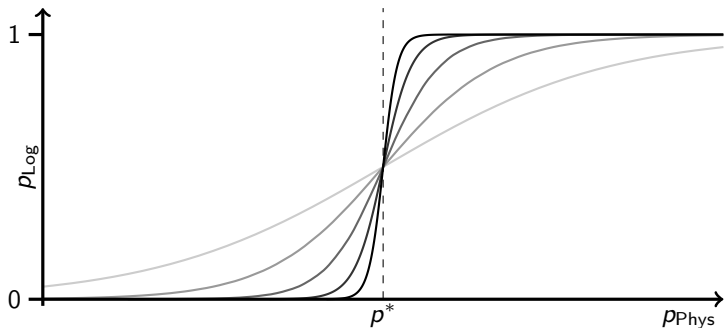
For large system sizes, performance is largely described by the threshold.



The inherent performance of the code can be studied by considering the optimal decoder.

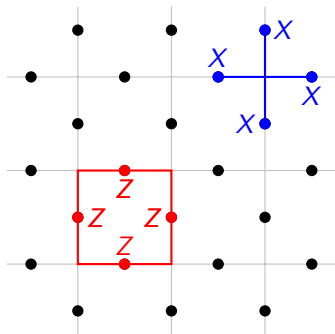
# Threshold

For large system sizes, performance is largely described by the threshold.



The inherent performance of the code can be studied by considering the optimal decoder.

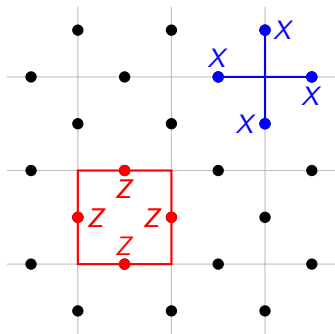
# Toric/surface code



The toric code admits a homological interpretation:

- Stabilisers form closed loops
- Logical operators form non-contractible loops
- Errors correspond to open paths
- Syndrome bits corresponds to the ends of paths

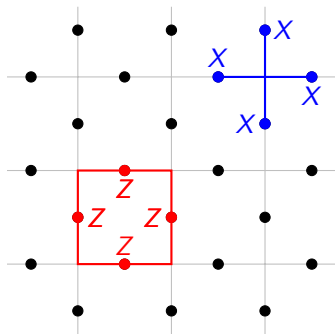
# Toric/surface code



The toric code admits a homological interpretation:

- Stabilisers form closed loops
- Logical operators form non-contractible loops
- Errors correspond to open paths
- Syndrome bits corresponds to the ends of paths

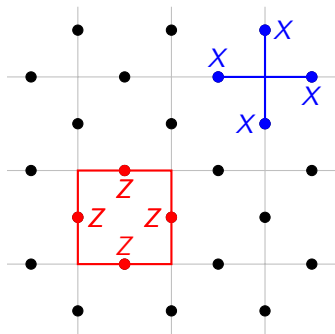
# Toric/surface code



The toric code admits a homological interpretation:

- Stabilisers form closed loops
- Logical operators form non-contractible loops
- Errors correspond to open paths
- Syndrome bits corresponds to the ends of paths

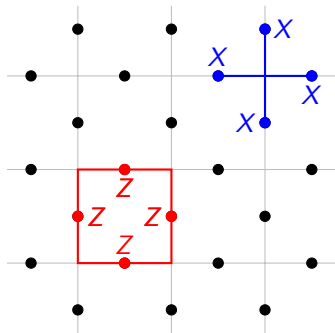
# Toric/surface code



The toric code admits a homological interpretation:

- Stabilisers form closed loops
- Logical operators form non-contractible loops
- Errors correspond to open paths
- Syndrome bits corresponds to the ends of paths

# Toric/surface code

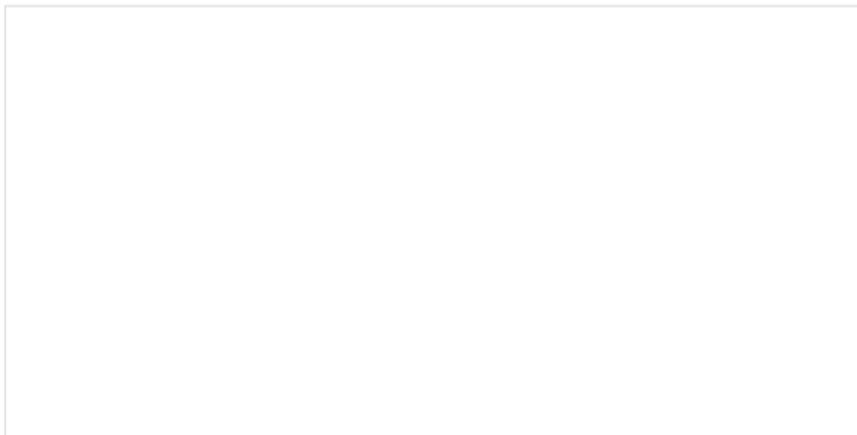


The toric code admits a homological interpretation:

- Stabilisers form closed loops
- Logical operators form non-contractible loops
- Errors correspond to open paths
- Syndrome bits corresponds to the ends of paths

# Pair matching decoder

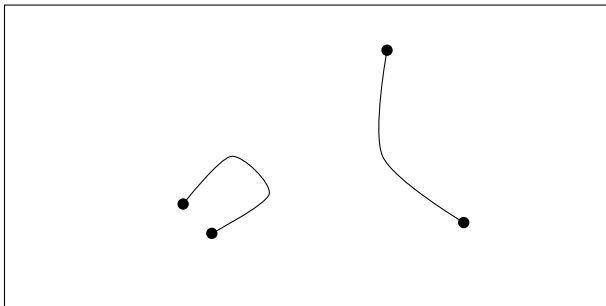
If errors are open paths, why not just close them? This leads to the pair matching decoder.



This decoder is efficient, but its slightly suboptimal for bit-flip and phase-flip errors, and performs badly for other errors.

# Pair matching decoder

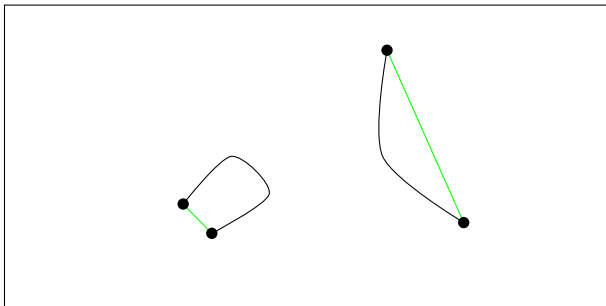
If errors are open paths, why not just close them? This leads to the pair matching decoder.



This decoder is efficient, but its slightly suboptimal for bit-flip and phase-flip errors, and performs badly for other errors.

# Pair matching decoder

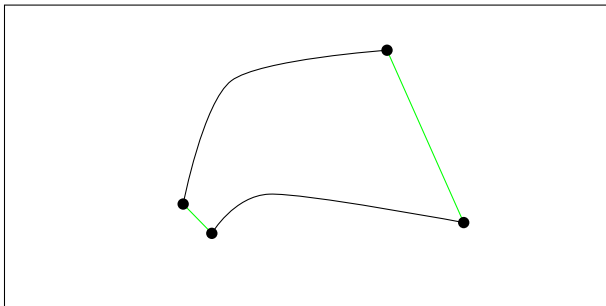
If errors are open paths, why not just close them? This leads to the pair matching decoder.



This decoder is efficient, but its slightly suboptimal for bit-flip and phase-flip errors, and performs badly for other errors.

# Pair matching decoder

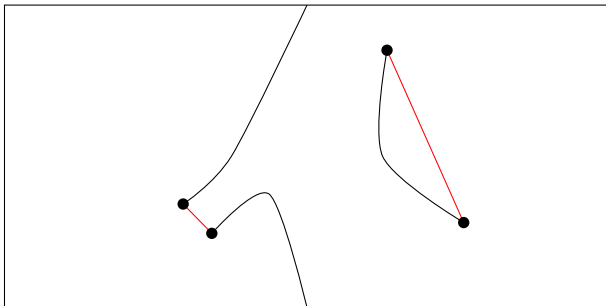
If errors are open paths, why not just close them? This leads to the pair matching decoder.



This decoder is efficient, but its slightly suboptimal for bit-flip and phase-flip errors, and performs badly for other errors.

# Pair matching decoder

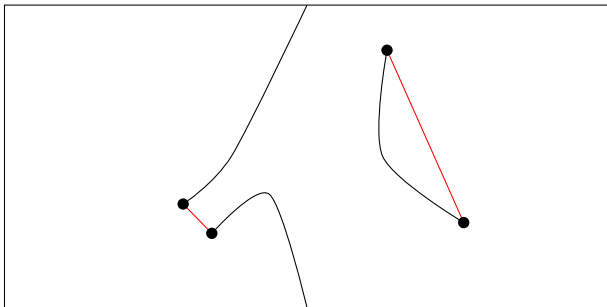
If errors are open paths, why not just close them? This leads to the pair matching decoder.



This decoder is efficient, but its slightly suboptimal for bit-flip and phase-flip errors, and performs badly for other errors.

# Pair matching decoder

If errors are open paths, why not just close them? This leads to the pair matching decoder.



This decoder is efficient, but its slightly suboptimal for bit-flip and phase-flip errors, and performs badly for other errors.

# Most likely error versus maximum likelihood

Why is pair matching suboptimal? In short, degeneracy.

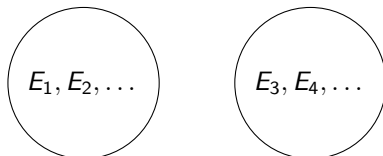
For quantum codes multiple errors can have the same syndrome. A decoder needs to identify the most likely error class, not the single most likely error.



# Most likely error versus maximum likelihood

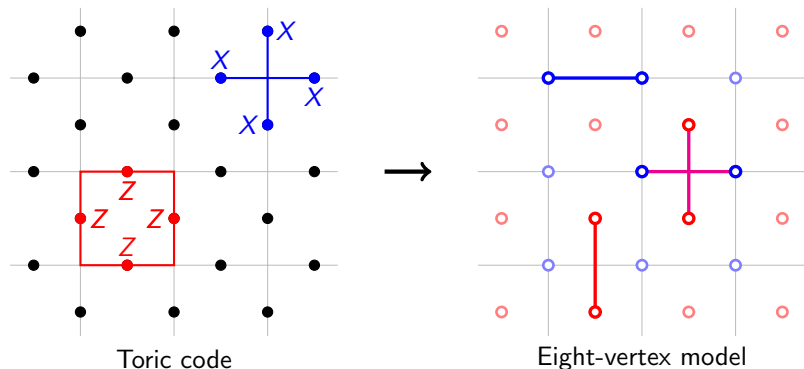
Why is pair matching suboptimal? In short, degeneracy.

For quantum codes multiple errors can have the same syndrome. A decoder needs to identify the most likely error class, not the single most likely error.



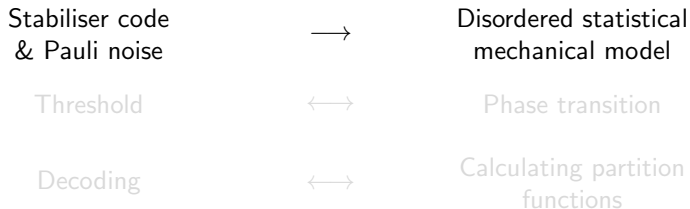
# Statistical mechanical mapping

The idea here is to construct a family of statistical mechanical models, whose thermodynamic properties reflect the error correction properties of the code.



This will allow us to use the analytic and numerical tools developed to study stat mech systems to study quantum codes.

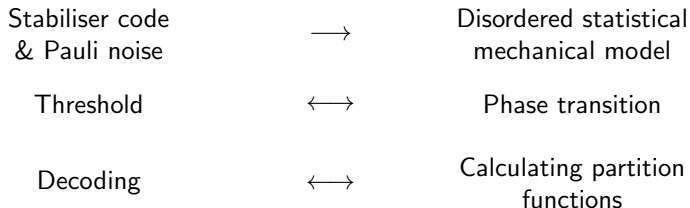
# Statistical mechanical mapping



Allows us to reappropriate techniques for studying stat. mech. systems to study quantum codes, e.g.



# Statistical mechanical mapping



Allows us to reappropriate techniques for studying stat. mech. systems to study quantum codes, e.g.



# Statistical mechanical mapping

Stabiliser code & Pauli noise	→	Disordered statistical mechanical model
Threshold	↔	Phase transition
Decoding	↔	Calculating partition functions

Allows us to reappropriate techniques for studying stat. mech. systems to study quantum codes, e.g.

Threshold approximation	←	Monte Carlo simulation
Optimal decoding	←	Partition function calculation

# Stabiliser codes and Pauli noise

For qubits, the Paulis  $\mathcal{P} := \{I, X, Y, Z\}$  are defined

$$I := \begin{pmatrix} 1 & 0 \\ 0 & 1 \end{pmatrix}, \quad X := \begin{pmatrix} 0 & 1 \\ 1 & 0 \end{pmatrix}, \quad Y := \begin{pmatrix} 0 & -i \\ i & 0 \end{pmatrix}, \quad Z := \begin{pmatrix} 1 & 0 \\ 0 & -1 \end{pmatrix}.$$

We will be considering stabiliser codes, which are specified by an Abelian subgroup of the Paulis  $\mathcal{S}$ , and whose code space  $\mathcal{C}$  is the joint  $+1$  eigenspace,

$$\mathcal{C} = \left\{ |\psi\rangle \mid S|\psi\rangle = |\psi\rangle, \forall S \in \mathcal{S} \right\}.$$

Any two errors which differ by a stabiliser are logically equivalent, so the logical classes of errors are

$$\bar{E} := \{ES \mid S \in \mathcal{S}\}$$

# Independent case: Hamiltonian

Let  $\llbracket A, B \rrbracket$  be the scalar commutator of two Paulis, such that  $AB =: \llbracket A, B \rrbracket BA$ .

For a stabiliser code generated by  $\{S_k\}_k$ , and an error Pauli  $E$ , the (disordered) Hamiltonian  $H_E$  is defined

$$H_E(\vec{s}) := - \sum_i \sum_{\sigma \in \mathcal{P}_i} \overbrace{J_i(\sigma)}^{\text{Coupling}} \overbrace{\llbracket \sigma, E \rrbracket}^{\text{Disorder}} \overbrace{\prod_{k: \llbracket \sigma, S_k \rrbracket = -1} s_k}^{\text{DoF}}$$

for  $s_k = \pm 1$ , and coupling strengths  $J_i(\sigma) \in \mathbb{R}$ .

Take-aways:

- Ising-type, with interactions corresponding to single-site Paulis  $\sigma$
- Disorder  $E$  flips some interactions (Ferro  $\leftrightarrow$  Anti-ferro)
- Local code  $\implies$  local stat. mech. model

# Independent case: Hamiltonian

Let  $\llbracket A, B \rrbracket$  be the scalar commutator of two Paulis, such that  $AB =: \llbracket A, B \rrbracket BA$ .

For a stabiliser code generated by  $\{S_k\}_k$ , and an error Pauli  $E$ , the (disordered) Hamiltonian  $H_E$  is defined

$$H_E(\vec{s}) := - \sum_i \sum_{\sigma \in \mathcal{P}_i} \overbrace{J_i(\sigma)}^{\text{Coupling}} \overbrace{\llbracket \sigma, E \rrbracket}^{\text{Disorder}} \overbrace{\prod_{k: \llbracket \sigma, S_k \rrbracket = -1} s_k}^{\text{DoF}}$$

for  $s_k = \pm 1$ , and coupling strengths  $J_i(\sigma) \in \mathbb{R}$ .

Take-aways:

- Ising-type, with interactions corresponding to single-site Paulis  $\sigma$
- Disorder  $E$  flips some interactions (Ferro  $\leftrightarrow$  Anti-ferro)
- Local code  $\implies$  local stat. mech. model

# Independent case: Hamiltonian

Let  $\llbracket A, B \rrbracket$  be the scalar commutator of two Paulis, such that  $AB =: \llbracket A, B \rrbracket BA$ .

For a stabiliser code generated by  $\{S_k\}_k$ , and an error Pauli  $E$ , the (disordered) Hamiltonian  $H_E$  is defined

$$H_E(\vec{s}) := - \sum_i \sum_{\sigma \in \mathcal{P}_i} \overbrace{J_i(\sigma)}^{\text{Coupling}} \overbrace{\llbracket \sigma, E \rrbracket}^{\text{Disorder}} \overbrace{\prod_{k: \llbracket \sigma, S_k \rrbracket = -1} s_k}^{\text{DoF}}$$

for  $s_k = \pm 1$ , and coupling strengths  $J_i(\sigma) \in \mathbb{R}$ .

Take-aways:

- Ising-type, with interactions corresponding to single-site Paulis  $\sigma$
- Disorder  $E$  flips some interactions (Ferro  $\leftrightarrow$  Anti-ferro)
- Local code  $\implies$  local stat. mech. model

## Independent case: Gauge symmetry

$$H_E(\vec{s}) = - \sum_i \sum_{\sigma \in \mathcal{P}_i} J_i(\sigma) \llbracket \sigma, E \rrbracket \prod_{k: \llbracket \sigma, S_k \rrbracket = -1} s_k$$

Using  $\llbracket A, B \rrbracket \llbracket A, C \rrbracket = \llbracket A, BC \rrbracket$ , we see this system has a gauge symmetry

$$s_k \rightarrow -s_k \quad \text{and} \quad E \rightarrow ES_k.$$

This gauge symmetry will capture the logical equivalence of errors,  $Z_E = Z_{ES_k}$ .

## Independent case: Gauge symmetry

$$H_E(\vec{s}) = - \sum_i \sum_{\sigma \in \mathcal{P}_i} J_i(\sigma) \llbracket \sigma, E \rrbracket \prod_{k: \llbracket \sigma, S_k \rrbracket = -1} s_k$$

Using  $\llbracket A, B \rrbracket \llbracket A, C \rrbracket = \llbracket A, BC \rrbracket$ , we see this system has a gauge symmetry

$$s_k \rightarrow -s_k \quad \text{and} \quad E \rightarrow ES_k.$$

This gauge symmetry will capture the logical equivalence of errors,  $Z_E = Z_{ES_k}$ .

# Independent case: Nishimori condition

Suppose we have an independent error model

$$\Pr(E) = \prod_i p_i(E_i),$$

we now want  $Z_E = \Pr(\bar{E})$ .

Using the gauge symmetry we have that the partition function can be written as a sum stabiliser-equivalent errors

$$Z_E = \sum_{\vec{s}} e^{-\beta H_E(\vec{s})} = \sum_S e^{-\beta H_{ES}(\vec{1})} = \sum_{F \in \bar{E}} e^{-\beta H_F(\vec{1})}.$$

If we select the coupling strength such that  $e^{-\beta H_E(\vec{1})} = \Pr(E)$ , then  $Z_E = \Pr(\bar{E})$  will follow.

# Independent case: Nishimori condition

Suppose we have an independent error model

$$\Pr(E) = \prod_i p_i(E_i),$$

we now want  $Z_E = \Pr(\bar{E})$ .

Using the gauge symmetry we have that the partition function can be written as a sum stabiliser-equivalent errors

$$Z_E = \sum_{\vec{s}} e^{-\beta H_E(\vec{s})} = \sum_S e^{-\beta H_{ES}(\vec{1})} = \sum_{F \in \bar{E}} e^{-\beta H_F(\vec{1})}.$$

If we select the coupling strength such that  $e^{-\beta H_E(\vec{1})} = \Pr(E)$ , then  $Z_E = \Pr(\bar{E})$  will follow.

# Independent case: Nishimori condition

Suppose we have an independent error model

$$\Pr(E) = \prod_i p_i(E_i),$$

we now want  $Z_E = \Pr(\bar{E})$ .

Using the gauge symmetry we have that the partition function can be written as a sum stabiliser-equivalent errors

$$Z_E = \sum_{\vec{s}} e^{-\beta H_E(\vec{s})} = \sum_S e^{-\beta H_{ES}(\vec{1})} = \sum_{F \in \bar{E}} e^{-\beta H_F(\vec{1})}.$$

If we select the coupling strength such that  $e^{-\beta H_E(\vec{1})} = \Pr(E)$ , then  $Z_E = \Pr(\bar{E})$  will follow.

## Independent case: Nishimori condition

We now want to pick our couplings such that  $e^{-\beta H_E(\vec{1})} = \Pr(E)$ . Expanding this out, we get

$$\sum_i \log p_i(E) = - \sum_i \sum_{\sigma} \beta J_i(\sigma) \llbracket \sigma, E \rrbracket.$$

Using the Fourier-like orthogonality relation  $\frac{1}{4} \sum_{\sigma} \llbracket \sigma, \tau \rrbracket = \delta_{\tau, I}$ , this becomes

Nishimori condition: 
$$\beta J_i(\sigma) = \frac{1}{4} \sum_{\tau \in \mathcal{P}} \log p_i(\tau) \llbracket \sigma, \tau \rrbracket,$$

which implies  $e^{-\beta H_E(\vec{1})} = \Pr(E)$ , and therefore  $Z_E = \Pr(\vec{E})$ .

This intrinsically links the error correcting behaviour of the code to the thermodynamic behaviour of the model (along the Nishimori line).

## Independent case: Nishimori condition

We now want to pick our couplings such that  $e^{-\beta H_E(\vec{1})} = \Pr(E)$ . Expanding this out, we get

$$\sum_i \log p_i(E) = - \sum_i \sum_{\sigma} \beta J_i(\sigma) \llbracket \sigma, E \rrbracket.$$

Using the Fourier-like orthogonality relation  $\frac{1}{4} \sum_{\sigma} \llbracket \sigma, \tau \rrbracket = \delta_{\tau, I}$ , this becomes

Nishimori condition: 
$$\beta J_i(\sigma) = \frac{1}{4} \sum_{\tau \in \mathcal{P}} \log p_i(\tau) \llbracket \sigma, \tau \rrbracket,$$

which implies  $e^{-\beta H_E(\vec{1})} = \Pr(E)$ , and therefore  $Z_E = \Pr(\bar{E})$ .

This intrinsically links the error correcting behaviour of the code to the thermodynamic behaviour of the model (along the Nishimori line).

## Independent case: Nishimori condition

We now want to pick our couplings such that  $e^{-\beta H_E(\vec{1})} = \Pr(E)$ . Expanding this out, we get

$$\sum_i \log p_i(E) = - \sum_i \sum_{\sigma} \beta J_i(\sigma) \llbracket \sigma, E \rrbracket.$$

Using the Fourier-like orthogonality relation  $\frac{1}{4} \sum_{\sigma} \llbracket \sigma, \tau \rrbracket = \delta_{\tau, I}$ , this becomes

Nishimori condition: 
$$\beta J_i(\sigma) = \frac{1}{4} \sum_{\tau \in \mathcal{P}} \log p_i(\tau) \llbracket \sigma, \tau \rrbracket,$$

which implies  $e^{-\beta H_E(\vec{1})} = \Pr(E)$ , and therefore  $Z_E = \Pr(\bar{E})$ .

This intrinsically links the error correcting behaviour of the code to the thermodynamic behaviour of the model (along the Nishimori line).

# Toric code and the random-bond Ising model

## Step 0: Code and noise model

### Toric code with iid bit-flips

#### Step 1: Degrees of freedom

$$s_v = \pm 1 \text{ on each vertex } v$$

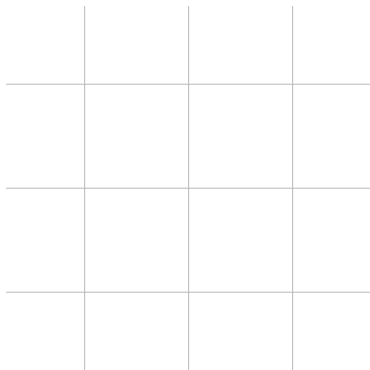
#### Step 2: Interactions

$$H_I = - \sum_{v \sim v'} J s_v s_{v'}$$

#### Step 3: Disorder

$$H_E = - \sum_{v \sim v'} J e_{vv'} s_v s_{v'}$$

$$\text{where } e_{vv'} = \begin{cases} +1 & E_{vv'} = I, \\ -1 & E_{vv'} = X. \end{cases}$$



# Toric code and the random-bond Ising model

Step 0: Code and noise model

Toric code with iid bit-flips

Step 1: Degrees of freedom

$$s_v = \pm 1 \text{ on each vertex } v$$

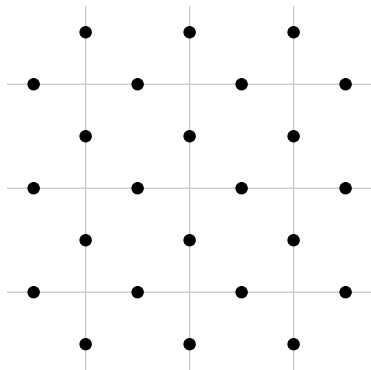
Step 2: Interactions

$$H_I = - \sum_{v \sim v'} J s_v s_{v'}$$

Step 3: Disorder

$$H_E = - \sum_{v \sim v'} J e_{vv'} s_v s_{v'}$$

$$\text{where } e_{vv'} = \begin{cases} +1 & E_{vv'} = I, \\ -1 & E_{vv'} = X. \end{cases}$$



# Toric code and the random-bond Ising model

## Step 0: Code and noise model

### Toric code with iid bit-flips

## Step 1: Degrees of freedom

$$s_v = \pm 1 \text{ on each vertex } v$$

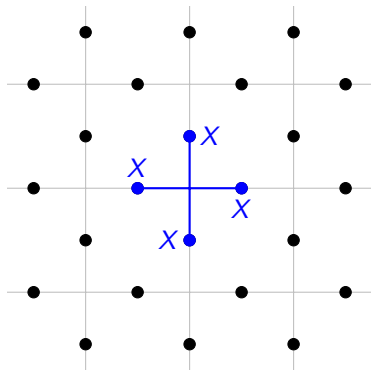
## Step 2: Interactions

$$H_I = - \sum_{v \sim v'} J s_v s_{v'}$$

## Step 3: Disorder

$$H_E = - \sum_{v \sim v'} J e_{vv'} s_v s_{v'}$$

$$\text{where } e_{vv'} = \begin{cases} +1 & E_{vv'} = I, \\ -1 & E_{vv'} = X. \end{cases}$$



# Toric code and the random-bond Ising model

## Step 0: Code and noise model

Toric code with iid bit-flips

$$\Pr(X_e) = p, \quad \Pr(I_e) = 1 - p.$$

## Step 1: Degrees of freedom

$$s_v = \pm 1 \text{ on each vertex } v$$

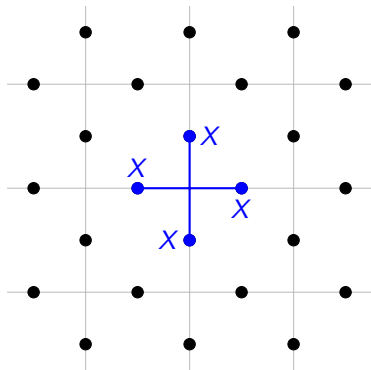
## Step 2: Interactions

$$H_I = - \sum_{v \sim v'} J s_v s_{v'}$$

## Step 3: Disorder

$$H_E = - \sum_{v \sim v'} J e_{vv'} s_v s_{v'}$$

$$\text{where } e_{vv'} = \begin{cases} +1 & E_{vv'} = I, \\ -1 & E_{vv'} = X. \end{cases}$$



# Toric code and the random-bond Ising model

Step 0: Code and noise model

Toric code with iid bit-flips

$$\Pr(X_e) = p, \quad \Pr(I_e) = 1 - p.$$

Step 1: Degrees of freedom

$$s_v = \pm 1 \text{ on each vertex } v$$

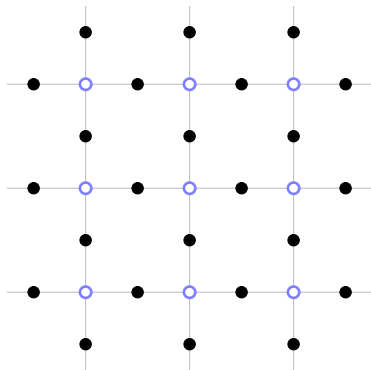
Step 2: Interactions

$$H_I = - \sum_{v \sim v'} J s_v s_{v'}$$

Step 3: Disorder

$$H_E = - \sum_{v \sim v'} J e_{vv'} s_v s_{v'}$$

$$\text{where } e_{vv'} = \begin{cases} +1 & E_{vv'} = I, \\ -1 & E_{vv'} = X. \end{cases}$$



# Toric code and the random-bond Ising model

Step 0: Code and noise model

Toric code with iid bit-flips

$$\Pr(X_e) = p, \quad \Pr(I_e) = 1 - p.$$

Step 1: Degrees of freedom

$$s_v = \pm 1 \text{ on each vertex } v$$

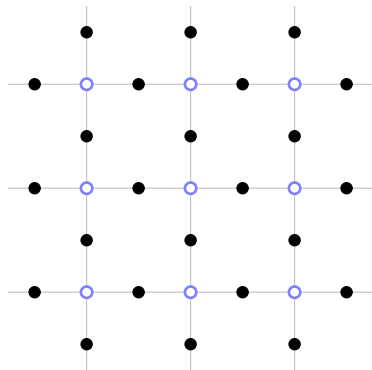
Step 2: Interactions

$$H_I = - \sum_{v \sim v'} J s_v s_{v'}$$

Step 3: Disorder

$$H_E = - \sum_{v \sim v'} J e_{vv'} s_v s_{v'}$$

$$\text{where } e_{vv'} = \begin{cases} +1 & E_{vv'} = I, \\ -1 & E_{vv'} = X. \end{cases}$$



# Toric code and the random-bond Ising model

Step 0: Code and noise model

Toric code with iid bit-flips

$$\Pr(X_e) = p, \quad \Pr(I_e) = 1 - p.$$

Step 1: Degrees of freedom

$s_v = \pm 1$  on each vertex  $v$

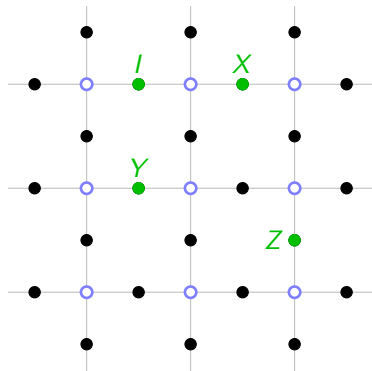
Step 2: Interactions

$$H_I = - \sum_{v \sim v'} J_{S_v S_{v'}}$$

Step 3: Disorder

$$H_E = - \sum_{v \sim v'} J_{e_{vv'}} s_v s_{v'}$$

$$\text{where } e_{vv'} = \begin{cases} +1 & E_{vv'} = I, \\ -1 & E_{vv'} = X. \end{cases}$$



$$[[\sigma_e, S_v]] = \begin{cases} -1 & \text{if } \sigma = Y, Z, v \in e, \\ +1 & \text{else.} \end{cases}$$

# Toric code and the random-bond Ising model

Step 0: Code and noise model

Toric code with iid bit-flips

$$\Pr(X_e) = p, \quad \Pr(I_e) = 1 - p.$$

Step 1: Degrees of freedom

$$s_v = \pm 1 \text{ on each vertex } v$$

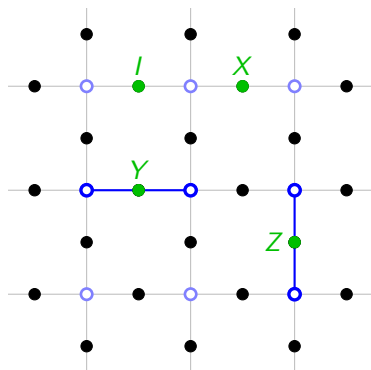
Step 2: Interactions

$$H_I = - \sum_{v \sim v'} J_{S_v S_{v'}}$$

Step 3: Disorder

$$H_E = - \sum_{v \sim v'} J_{e_{vv'}} s_v s_{v'}$$

$$\text{where } e_{vv'} = \begin{cases} +1 & E_{vv'} = I, \\ -1 & E_{vv'} = X. \end{cases}$$



$$[[\sigma_e, S_v]] = \begin{cases} -1 & \text{if } \sigma = Y, Z, v \in e, \\ +1 & \text{else.} \end{cases}$$

# Toric code and the random-bond Ising model

Step 0: Code and noise model

Toric code with iid bit-flips

$$\Pr(X_e) = p, \quad \Pr(I_e) = 1 - p.$$

Step 1: Degrees of freedom

$$s_v = \pm 1 \text{ on each vertex } v$$

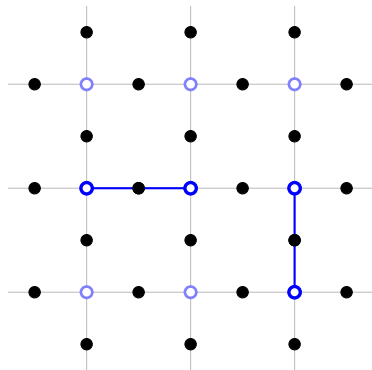
Step 2: Interactions

$$H_I = - \sum_{v \sim v'} J s_v s_{v'}$$

Step 3: Disorder

$$H_E = - \sum_{v \sim v'} J e_{vv'} s_v s_{v'}$$

$$\text{where } e_{vv'} = \begin{cases} +1 & E_{vv'} = I, \\ -1 & E_{vv'} = X. \end{cases}$$



# Toric code and the random-bond Ising model

Step 0: Code and noise model

Toric code with iid bit-flips

$$\Pr(X_e) = p, \quad \Pr(I_e) = 1 - p.$$

Step 1: Degrees of freedom

$$s_v = \pm 1 \text{ on each vertex } v$$

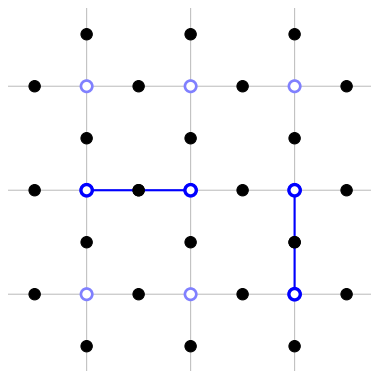
Step 2: Interactions

$$H_I = - \sum_{v \sim v'} J s_v s_{v'}$$

Step 3: Disorder

$$H_E = - \sum_{v \sim v'} J e_{vv'} s_v s_{v'}$$

$$\text{where } e_{vv'} = \begin{cases} +1 & E_{vv'} = I, \\ -1 & E_{vv'} = X. \end{cases}$$



$$[[\sigma, S_k]] \rightarrow [[\sigma, ES_k]]$$

# Toric code and the random-bond Ising model

Step 0: Code and noise model

Toric code with iid bit-flips

$$\Pr(X_e) = p, \quad \Pr(I_e) = 1 - p.$$

Step 1: Degrees of freedom

$$s_v = \pm 1 \text{ on each vertex } v$$

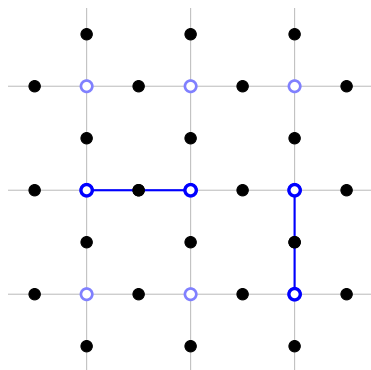
Step 2: Interactions

$$H_I = - \sum_{v \sim v'} J s_v s_{v'}$$

Step 3: Disorder

$$H_E = - \sum_{v \sim v'} J e_{vv'} s_v s_{v'}$$

$$\text{where } e_{vv'} = \begin{cases} +1 & E_{vv'} = I, \\ -1 & E_{vv'} = X. \end{cases}$$



$$[[\sigma, S_k]] \rightarrow [[\sigma, ES_k]]$$

# Toric code and the random-bond Ising model

Step 0: Code and noise model

Toric code with iid bit-flips

Step 1: Degrees of freedom

$s_v = \pm 1$  on each vertex  $v$

Step 2: Interactions

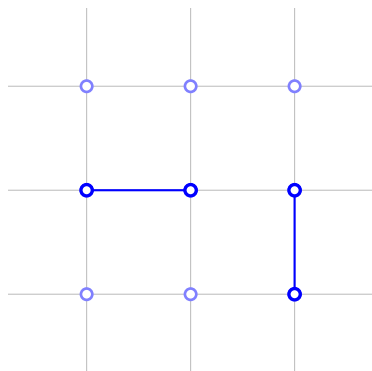
$$H_I = - \sum_{v \sim v'} J s_v s_{v'}$$

Step 3: Disorder

$$H_E = - \sum_{v \sim v'} J e_{vv'} s_v s_{v'}$$

$$\text{where } e_{vv'} = \begin{cases} +1 & E_{vv'} = I, \\ -1 & E_{vv'} = X. \end{cases}$$

$$\Pr(+J) = p, \quad \Pr(-J) = 1 - p.$$



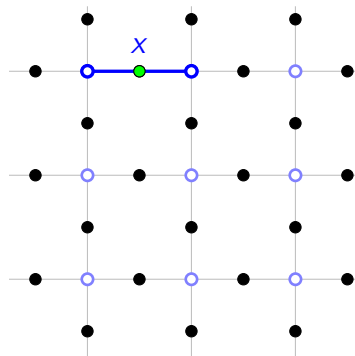
$\pm J$  Random-bond Ising Model

# Other independent examples

## Toric code

Bit-flip  $\rightarrow$  Random-bond Ising<sup>1</sup>

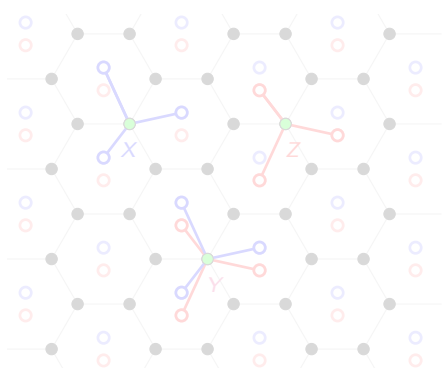
Indep.  $X$  &  $Z \rightarrow 2 \times$  Random-bond Ising  
Depolarising  $\rightarrow$  Random 8-vertex model<sup>2</sup>



## Colour code

Bit-flip  $\rightarrow$  Random 3-spin Ising

Indep.  $X$  &  $Z \rightarrow 2 \times$  Random 3-spin Ising  
Depolarising  $\rightarrow$  Random interacting 8-vertex<sup>2</sup>



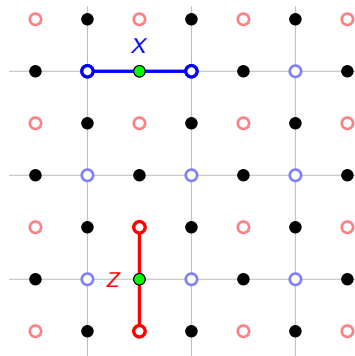
<sup>1</sup>Dennis et.al., JMP 2002, doi:10/cs2mtf, arXiv:quant-ph/0110143

<sup>2</sup>Bombin et.al., PRX 2012, doi:10/crz5, arXiv:1202.1852

# Other independent examples

## Toric code

Bit-flip  $\rightarrow$  Random-bond Ising<sup>1</sup>  
Indep. X&Z  $\rightarrow$  2 $\times$ Random-bond Ising  
Depolarising  $\rightarrow$  Random 8-vertex model<sup>2</sup>



## Colour code

Bit-flip  $\rightarrow$  Random 3-spin Ising  
Indep. X&Z  $\rightarrow$  2 $\times$ Random 3-spin Ising  
Depolarising  $\rightarrow$  Random interacting 8-vertex<sup>2</sup>



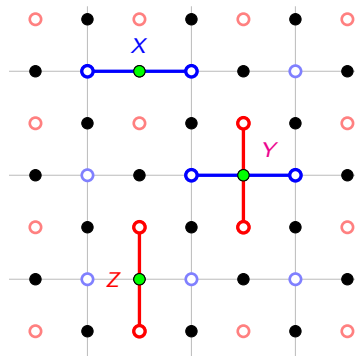
<sup>1</sup>Dennis et.al., JMP 2002, doi:10/cs2mtf, arXiv:quant-ph/0110143

<sup>2</sup>Bombin et.al., PRX 2012, doi:10/crz5, arXiv:1202.1852

# Other independent examples

## Toric code

Bit-flip  $\rightarrow$  Random-bond Ising<sup>1</sup>  
Indep. X&Z  $\rightarrow$  2 $\times$ Random-bond Ising  
Depolarising  $\rightarrow$  Random 8-vertex model<sup>2</sup>



## Colour code

Bit-flip  $\rightarrow$  Random 3-spin Ising  
Indep. X&Z  $\rightarrow$  2 $\times$ Random 3-spin Ising  
Depolarising  $\rightarrow$  Random interacting 8-vertex<sup>2</sup>



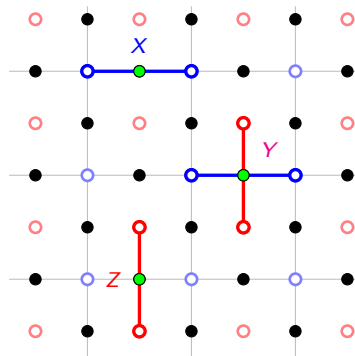
<sup>1</sup>Dennis et.al., JMP 2002, doi:10/cs2mtf, arXiv:quant-ph/0110143

<sup>2</sup>Bombin et.al., PRX 2012, doi:10/crz5, arXiv:1202.1852

# Other independent examples

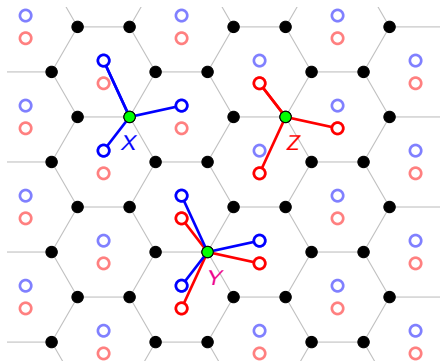
## Toric code

Bit-flip  $\rightarrow$  Random-bond Ising<sup>1</sup>  
Indep.  $X$  &  $Z \rightarrow 2 \times$  Random-bond Ising  
Depolarising  $\rightarrow$  Random 8-vertex model<sup>2</sup>



## Colour code

Bit-flip  $\rightarrow$  Random 3-spin Ising  
Indep.  $X$  &  $Z \rightarrow 2 \times$  Random 3-spin Ising  
Depolarising  $\rightarrow$  Random interacting 8-vertex<sup>2</sup>



<sup>1</sup>Dennis et.al., JMP 2002, doi:10/cs2mtf, arXiv:quant-ph/0110143

<sup>2</sup>Bombin et.al., PRX 2012, doi:10/crz5, arXiv:1202.1852

# Error correction threshold as a quenched phase transition

Consider the free energy cost of a logical error  $L$ ,

$$\Delta_E(L) = -\frac{1}{\beta} \log Z_{EL} + \frac{1}{\beta} \log Z_E.$$

Along the Nishimori line

$$\Delta_E(L) = \frac{1}{\beta} \log \frac{\Pr(\bar{E})}{\Pr(EL)},$$

which implies

Below threshold :  $\Delta_E(L) \rightarrow \infty$  (in mean)

Above threshold :  $\Delta_E(L) \rightarrow 0$  (in prob.)

# Error correction threshold as a quenched phase transition

Consider the free energy cost of a logical error  $L$ ,

$$\Delta_E(L) = -\frac{1}{\beta} \log Z_{EL} + \frac{1}{\beta} \log Z_E.$$

Along the Nishimori line

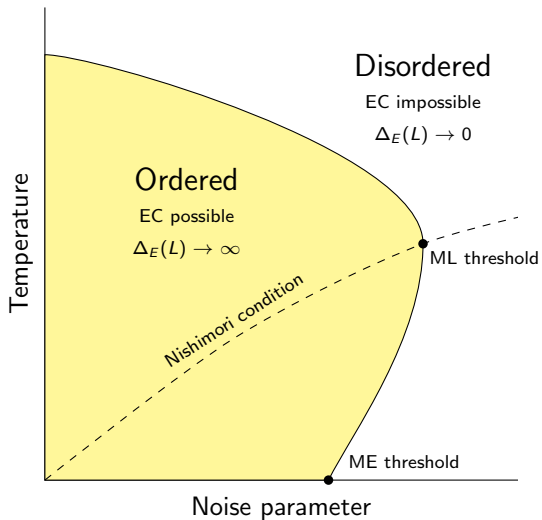
$$\Delta_E(L) = \frac{1}{\beta} \log \frac{\Pr(\bar{E})}{\Pr(EL)},$$

which implies

Below threshold :  $\Delta_E(L) \rightarrow \infty$  (in mean)

Above threshold :  $\Delta_E(L) \rightarrow 0$  (in prob.)

# Phase diagram sketch



## Correlated case

The key point independence gave us was the ability to factor our noise model

$$\Pr(E) = \prod_i p_i(E_i).$$

We can generalise this to correlated models:

### Factored distribution

An error model factors over regions  $\{R_j\}_j$  if there exist  $\phi_j : \mathcal{P}_{R_j} \rightarrow \mathbb{R}$  such that

$$\Pr(E) = \prod_j \phi_j(E_{R_j})$$

This model includes many probabilistic graphical models, such as Bayesian Networks and Markov/Gibbs Random Fields.

## Correlated case

The key point independence gave us was the ability to factor our noise model

$$\Pr(E) = \prod_i p_i(E_i).$$

We can generalise this to correlated models:

### Factored distribution

An error model factors over regions  $\{R_j\}_j$  if there exist  $\phi_j : \mathcal{P}_{R_j} \rightarrow \mathbb{R}$  such that

$$\Pr(E) = \prod_j \phi_j(E_{R_j})$$

This model includes many probabilistic graphical models, such as Bayesian Networks and Markov/Gibbs Random Fields.

## Correlated case

By construction, we can extend to the correlated case by changing  $\sigma \in \mathcal{P}_i$  to  $\sigma \in \mathcal{P}_{R_j}$ :

$$H_E(\vec{s}) := - \sum_j \sum_{\sigma \in \mathcal{P}_{R_j}} J_j(\sigma) \llbracket \sigma, E \rrbracket \prod_{k: \llbracket \sigma, S_k \rrbracket = -1} s_k$$

Nishimori condition: 
$$\beta J_j(\sigma) = \frac{1}{|\mathcal{P}_{R_j}|} \sum_{\tau \in \mathcal{P}_{R_j}} \log \phi_j(\tau) \llbracket \sigma, \tau \rrbracket,$$

As before we get that  $Z_E = \Pr(\bar{E})$ , and so the threshold manifests as a phase transition.

## Correlated case

By construction, we can extend to the correlated case by changing  $\sigma \in \mathcal{P}_i$  to  $\sigma \in \mathcal{P}_{R_j}$ :

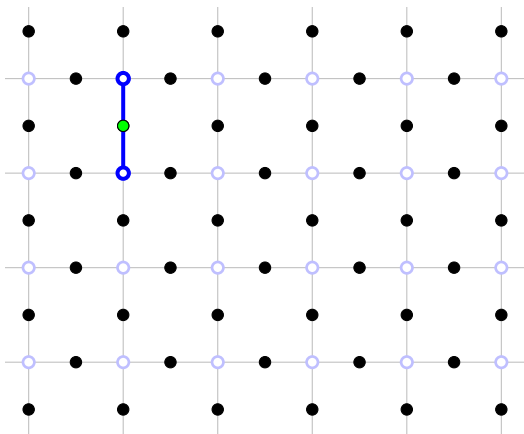
$$H_E(\vec{s}) := - \sum_j \sum_{\sigma \in \mathcal{P}_{R_j}} J_j(\sigma) \llbracket \sigma, E \rrbracket \prod_{k: \llbracket \sigma, S_k \rrbracket = -1} s_k$$

Nishimori condition: 
$$\beta J_j(\sigma) = \frac{1}{|\mathcal{P}_{R_j}|} \sum_{\tau \in \mathcal{P}_{R_j}} \log \phi_j(\tau) \llbracket \sigma, \tau \rrbracket,$$

As before we get that  $Z_E = \Pr(\bar{E})$ , and so the threshold manifests as a phase transition.

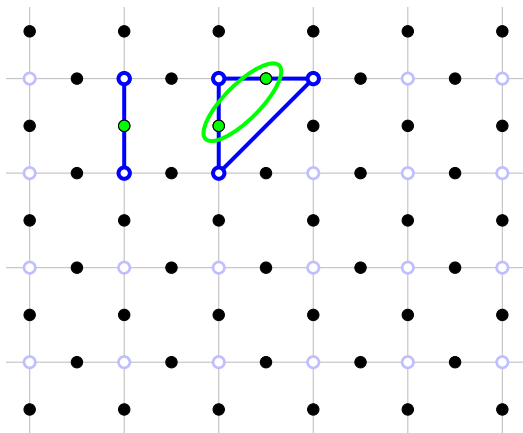
# Correlated example

**Toric code with correlated bit-flips**  
Correlations induce longer-range interactions



# Correlated example

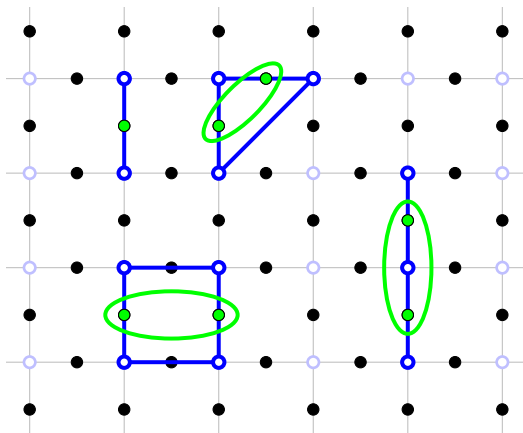
**Toric code with correlated bit-flips**  
Correlations induce longer-range interactions



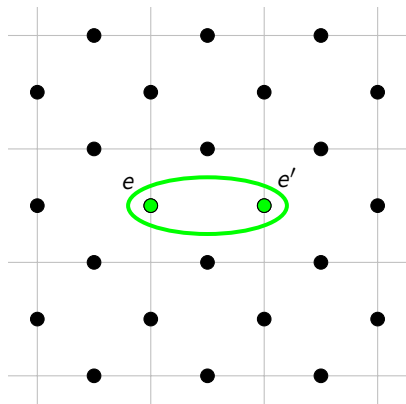


# Correlated example

**Toric code with correlated bit-flips**  
Correlations induce longer-range interactions



# 'Across plaquette' correlated bit-flips



This error model is entirely specified by the conditional error probabilities

$$\begin{array}{ll} \Pr(I_e|I_{e'}) & \Pr(I_e|X_{e'}) \\ \Pr(X_e|I_{e'}) & \Pr(X_e|X_{e'}) \end{array}$$

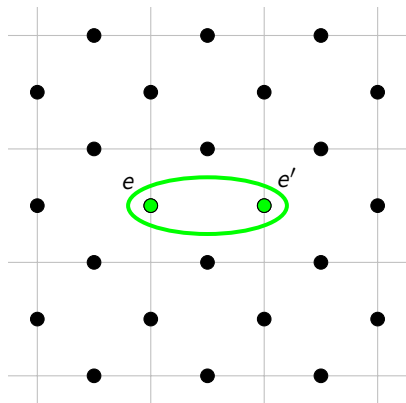
for all neighbouring edges  $e$  and  $e'$ .

For our purposes, it will be convenient to parameterise things by

$$p := \Pr(X_e), \quad \eta := \frac{\Pr(X_e|X_{e'})}{\Pr(X_e|I_{e'})}.$$

Here  $p$  is the marginal error rate, and  $\eta$  is a measure of the correlations.

# 'Across plaquette' correlated bit-flips



This error model is entirely specified by the conditional error probabilities

$$\begin{array}{ll} \Pr(I_e|I_{e'}) & \Pr(I_e|X_{e'}) \\ \Pr(X_e|I_{e'}) & \Pr(X_e|X_{e'}) \end{array}$$

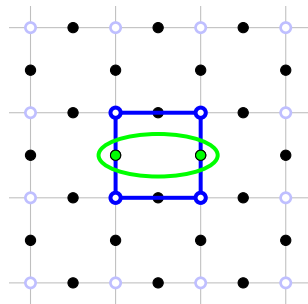
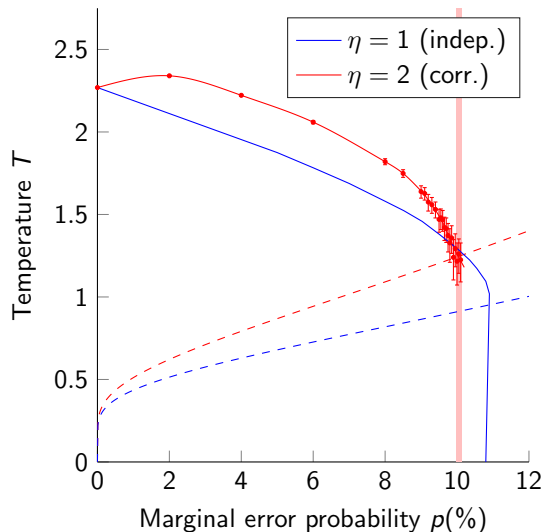
for all neighbouring edges  $e$  and  $e'$ .

For our purposes, it will be convenient to parameterise things by

$$p := \Pr(X_e), \quad \eta := \frac{\Pr(X_e|X_{e'})}{\Pr(X_e|I_{e'})}.$$

Here  $p$  is the marginal error rate, and  $\eta$  is a measure of the correlations.

# Monte Carlo simulations



## Thresholds

Indep.:  $p_{\text{th}} = 10.917(3)\%^{1,2}$

Corr.:  $p_{\text{th}} = 10.04(6)\%$

<sup>1</sup>Dennis et.al., JMP 2002, doi:10/cs2mtf, arXiv:quant-ph/0110143

<sup>2</sup>Toldin et.al., JSP 2009, doi:10/c3r2kc, arXiv:0811.2101

# Decoding from partition functions

Along the Nishimori line, the maximum likelihood condition corresponds to maximising the partition function

$$\ell = \arg \max_{\ell} Z_{EL\ell}.$$

Approximating  $Z_{EL\ell}$  therefore allows us to approximate the ML decoder.

- Step 1: Measure the syndrome  $s$
- Step 2: Construct an arbitrary error  $C_s$  which has syndrome  $s$
- Step 3: Approximate  $Z_{C_s L_l} = \Pr(\overline{C_s L_l})$  for each logical class  $l$
- Step 4: Find the  $l$  such that  $Z_{C_s L_l}$  is maximised
- Step 5: Apply  $(C_s L_l)^{-1}$

# Decoding from partition functions

Along the Nishimori line, the maximum likelihood condition corresponds to maximising the partition function

$$\ell = \arg \max_{\ell} Z_{EL\ell}.$$

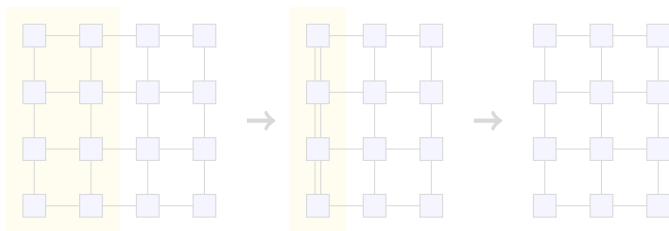
Approximating  $Z_{EL\ell}$  therefore allows us to approximate the ML decoder.

- Step 1: Measure the syndrome  $s$
- Step 2: Construct an arbitrary error  $C_s$  which has syndrome  $s$
- Step 3: Approximate  $Z_{C_s L_l} = \Pr(\overline{C_s L_l})$  for each logical class  $l$
- Step 4: Find the  $l$  such that  $Z_{C_s L_l}$  is maximised
- Step 5: Apply  $(C_s L_l)^{-1}$

# Decoding from (approximate) tensor network contraction

Partition functions can be expressed as tensor networks<sup>1,2</sup>, allowing us to use approximate tensor network contraction schemes.

For 2D codes and locally correlated noise, this tensor network is also 2D. Here we can use the MPS-MPO approximation contraction scheme considered by Bravyi, Suchara and Vargo<sup>3</sup>:



<sup>1</sup>Verstraete et. al., PRL 2006, doi:10/dfgcz8, arXiv:quant-ph/0601075

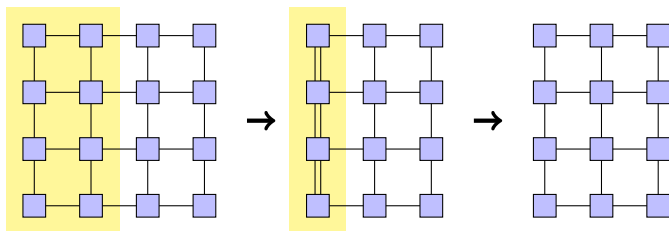
<sup>2</sup>Bridgeman and Chubb, JPA 2017, doi:10/cv7m, arXiv:1603.03039

<sup>3</sup>Bravyi, Scuhara, Vargo, PRA 2014, doi:10/cv7n, arXiv:1405.4883

# Decoding from (approximate) tensor network contraction

Partition functions can be expressed as tensor networks<sup>1,2</sup>, allowing us to use approximate tensor network contraction schemes.

For 2D codes and locally correlated noise, this tensor network is also 2D. Here we can use the MPS-MPO approximation contraction scheme considered by Bravyi, Suchara and Vargo<sup>3</sup>:



<sup>1</sup>Verstraete et. al., PRL 2006, doi:10/dfgcz8, arXiv:quant-ph/0601075

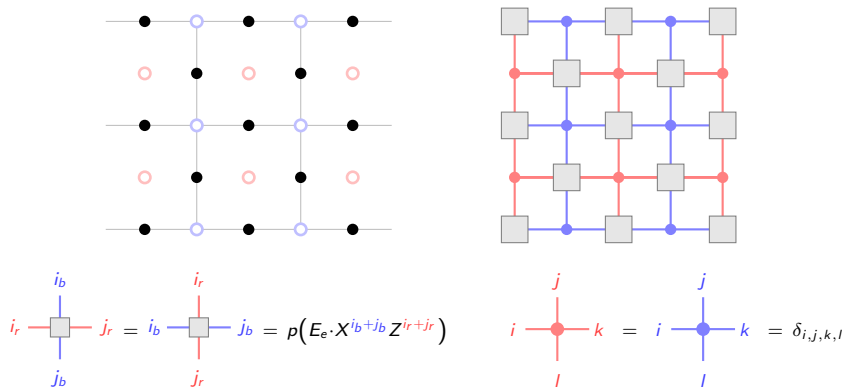
<sup>2</sup>Bridgeman and Chubb, JPA 2017, doi:10/cv7m, arXiv:1603.03039

<sup>3</sup>Bravyi, Scuhara, Vargo, PRA 2014, doi:10/cv7n, arXiv:1405.4883

# Decoding from (approximate) tensor network contraction

This gives an algorithm for (approximate) maximum likelihood decoding for any 2D code, subject to any locally correlated noise, generalising BSV.

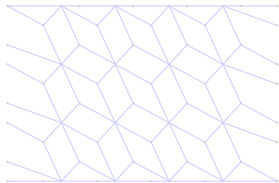
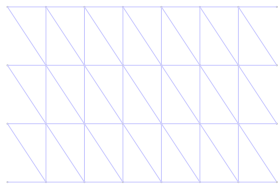
Indeed, applying this to iid noise in the surface code reproduces BSV:



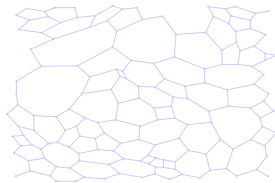
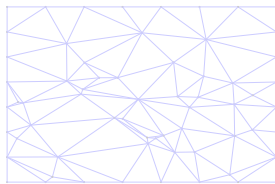
# Ongoing work: Surface codes on different graphs

The TN decoder lets us efficiently probe the threshold of 2D topological codes. What happens if we change the underlying graph?

Raise or lower the connectivity



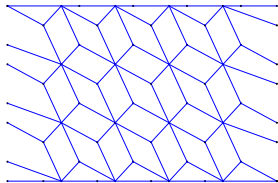
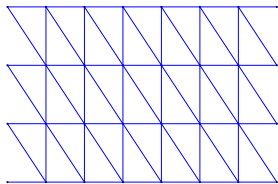
Irregular graphs



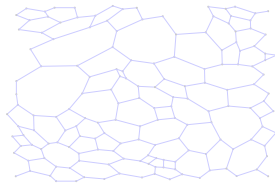
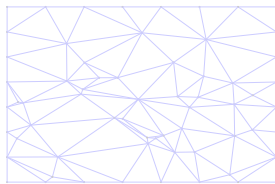
# Ongoing work: Surface codes on different graphs

The TN decoder lets us efficiently probe the threshold of 2D topological codes. What happens if we change the underlying graph?

Raise or lower the connectivity



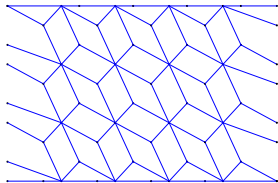
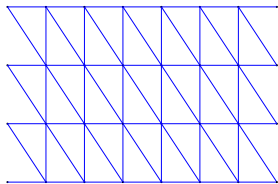
Irregular graphs



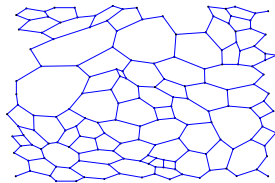
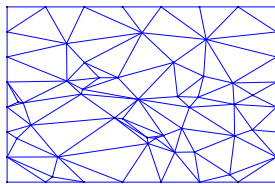
# Ongoing work: Surface codes on different graphs

The TN decoder lets us efficiently probe the threshold of 2D topological codes. What happens if we change the underlying graph?

Raise or lower the connectivity



Irregular graphs



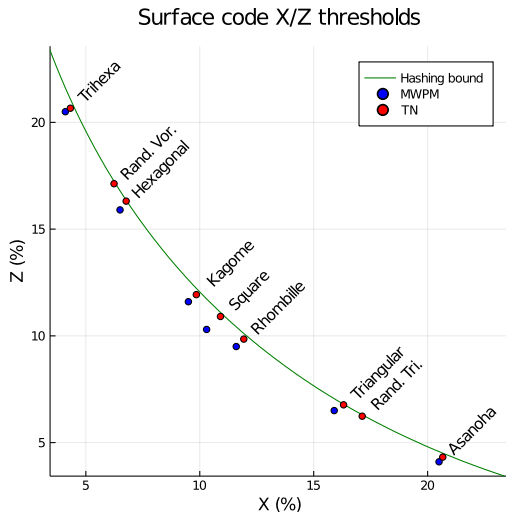
# Ongoing work: Surface codes on different graphs

We find a trade-off between the  $X$  and  $Z$  thresholds.

Hashing bound:  $h(p_x) + h(p_z) < 1$ .

Pair matching studied earlier by Fujii et.al.<sup>4</sup>

We are currently running similar numerics for depolarising noise, and the colour code.



<sup>4</sup>Fujii et.al., doi.org/d5sb, arXiv:1202.2743

- TN decoding of LDPCs (ongoing work with Stefanos Kourtis)
- Use TN decoder to design codes for correlated noise

# Thank you!

Stat Mech Mapping: arXiv:1809.10704, to appear in AIHPD  
Tensor Network decoding: To appear arXiv:2009:?????

✉ me@christopherchubb.com

🔗 christopherchubb.com

🐦 @QuantumChubb